

Exploration of Parameter Spaces Assisted by Machine Learning

A. Hammad^{1*}, Myeonghun Park^{1,2,3}, Raymundo Ramos^{1†} and Pankaj Saha^{1,2}

¹ Institute of Convergence Fundamental Studies, Seoultech, Seoul 01811, Korea

² School of Natural Sciences, Seoultech, Seoul 01811, Korea

³ School of Physics, KIAS, Seoul 02455, Korea

*ahhammad@cern.ch, †rayramosang@gmail.com

August 5, 2022

Abstract

We demonstrate two sampling procedures assisted by machine learning models via regression and classification. The objective is the construction of routines that can be employed for different types of analysis, from finding bounds on the parameter space to accumulating samples in areas of interest. Moreover, for classification, we introduce a boosting technique to improve cases where the initial convergence is slow. The type of results that can be obtained is better explained with the help of a few examples from sampling simple toy models to exploring the parameter space of the two Higgs doublet model. The code used for this paper and instructions are publicly available on the web¹.

Contents

1	Introduction	2
2	Machine Learning Assisted Parameter Space Finding	3
3	Application to toy models	5
3.1	Boosting the start up convergence	7
4	Learning the Higgs signal strength in 2HDM-II potential	8
4.1	The model	8
5	Conclusion	12
	References	14

¹<https://github.com/AHamamd150/MLscanner>

1 Introduction

Technological advancements bring computers with more powerful processing capabilities but at the same time bring more diverse, advanced and precise experimental probes. A considerable part of the scientific community is tasked with applying these powerful computers to adjust known and new theoretical models to the most up to date constraints found by experiments. This usually involves taking a set of free parameters from the model, calculate predictions for the observables that depend on them and comparing with the experiments of interest. Then we can judge the success of the model based on how well it can predict said observables within the experimental errors. One common starting point for new models is extending the model that works best, e.g., the standard model of particle physics for high energy physics (HEP) or the cold dark matter model with a cosmological constant (Λ CDM) for cosmology. Very minimal extensions may not provide enough freedom to explain deviations observed in experiments, thus, one may end with additions that increase the number of free parameters considerably. With an increase of parameters the number of points required for proper sampling increases exponentially. Multiplying this number by the time required to calculate an ever growing number of experimental constraints [1] can give an estimation of the required effective time.

Besides parallelizing the computations, to simplify and accelerate the task of exploring large parameter spaces (both in size of ranges and number of parameters), several methods have been devised. Two successful and well known examples are Markov chain Monte Carlo (MCMC) [2] and MultiNest [3, 4] (see Ref. [5–14] for examples of studies that use these tools). These tools are cleverly designed to reduce the time required to obtain precise limits on the parameters, when compared to scanning on a grid or random scan. Notwithstanding their usefulness and improvements, these tools are far from perfect and have some well known issues when tasked with finding complicated subspaces [15, 16].

Machine learning (ML) techniques are natural contenders for alleviating such difficulties for their ability to find concealed patterns in large and complex data sets (See Ref. [17] for a review and references therein). Recently, it was proposed a general purpose method known as ML Scan (MLS) [15, 18], where the authors use a deep neural network to iteratively probe the parameter space, starting with points randomly distributed, where the sampling is improved incrementally with active learning. Conversely, the active learning methods proposed in Refs. [16, 19] are based on finding *decision boundaries* of the allowed subspace. Application to HEP can be found in Ref. [20]. In Ref. [21], the authors introduce dynamic sampling techniques for beyond the standard model searches.

In this work, we have implemented two broad classes of ML based efficient sampling methods of parameter spaces, using regression and classification. Similarly to Refs. [15, 16, 18, 19], we employ an iterative process where the ML model is trained on a set of parameter values and their results from a costly calculation, with the same ML model later used to predict the location of additional relevant parameter values. The ML model is refined in every step of the process, therefore, increasing the accuracy of the regions it suggests. We attempt to develop a generic tool that can take advantage of the improvements brought by this iterative process. Differently to Refs. [16, 19], we set the goal in filling the regions of interest such that in the end we provide a sample of parameter values that densely spans the region as requested by the user. With enough points sampled, it should not be difficult to proceed with more detailed studies on the implications of the calculated observables and the validity of the model under question. We pay special attention to give control to the user over the many hyperparameters involved in the pro-

cess, such as the number of nodes, learning rate, training epochs, among many others, while also suggesting defaults that work in many cases. The user has the freedom to decide whether to use regression or classification to sample the parameter space, depending mostly on the complexity of the problem. For example, with complicated fast changing likelihoods it may be easier for a ML classifier to converge and suggest points that are likely inside the region of interest. However, with observables that are relatively easy to adjust, a ML regressor may provide information useful to locate points of interest such as best fit points, or to estimate the distribution of the parameters. After several steps in the iterative process, it is expected to have a ML model that can accurately predict the relevance of a parameter point much faster than passing through the complicated time consuming calculation that was used during training. As a caveat, considering that this process requires iteratively training a ML model during several epochs, which also requires time by itself, for cases where the calculations can be optimized to run rather fast, other methods may actually provide good results in less time.

The organization of this paper is as follows. In Sec. 2 we describe in detail the two iterative processes for sampling parameter spaces using regression and classification. We expand in Sec. 3 by applying said processes to two toy models in 2 and 3 dimensions, including a description of how we can boost the convergence of the ML model. In Sec. 4 we describe how we sample regions of interest of the two Higgs doublet model (2HDM) using well-known HEP packages and the processes described in this paper. In the end, we conclude with a summary of the most relevant details presented in this work.

2 Machine Learning Assisted Parameter Space Finding

The process starts with a set of random values, K_0 , for the parameters that will be scanned over, and their results from a calculation of observables, $Y(K_0)$. This random set of parameter values and their results are used to train a ML model with the purpose of predicting meaningful regions in successive iterations where the model will be further refined. After the initial (0^{th}) training step, we will follow an iterative process that, in its most basic form, is summarized with the following steps:

1. Use the ML model to obtain a prediction, \hat{Y} , for the output of a HEP calculation for a large set of random parameter values, L .
2. Based on this prediction, select a smaller set of points, K , using some criteria that depends on the type of analysis of interest. Up to this step we should have a set K and its corresponding predictions $\hat{Y}(K)$.
3. Pass the set K of parameter values to the HEP calculation to obtain the actual results $Y(K)$.
4. Use the set K and its results $Y(K)$ to refine the training of the ML model.
5. The loop closes when we use this refined model to predict the HEP calculation output for a larger set of parameter values as in step 1 above.

Later in the text and in specific examples we will expand on the implementation of these brief summary.

It is assumed that the calculation of the observables is done through an expensive, time consuming computation, such that it is worthwhile spending additional time training a ML model

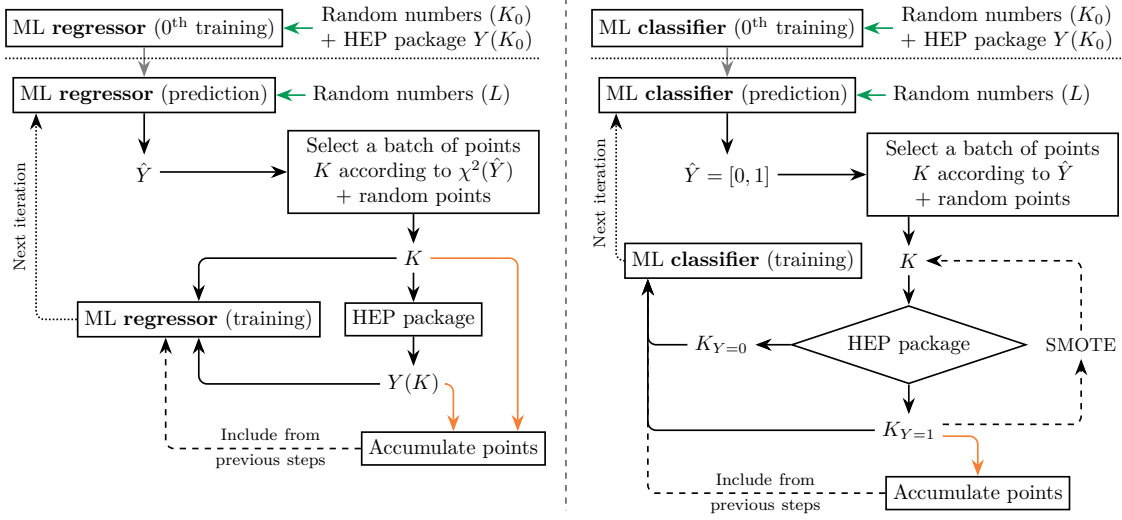


Figure 1: Charts for the ML iterative process used for the regressor (left) and the classifier (right). The main predict-train loop is indicated with black arrows, green arrows indicate places where a random number set is required and the orange arrow marks where we collect the output points. The points accumulated up to step n_k are added for training during step n_{k+1} .

with its results. Taking these basic steps as the starting point, one can further fill in the details of the sampling, considering that there is a number of ML models to choose from and that the selection of the set K depends highly on the region of interest. Regarding the choice of the set K , in general it is a good idea to add an amount of points chosen at random to enforce exploration of new parameter space regardless of the suggestion of the ML model. It is useful to gather the K set and the results from the HEP calculation in every iteration as they represent the sampling of the parameter space. For the training step we always use the new points from the corresponding iteration, but we have the choice to add all or some of the set of accumulated points. After a large amount of points have been accumulated training on the full set may be time consuming, therefore, it would be a good idea to devise rules on how to include them. For example, in Ref. [16] the full set of accumulated points is used to train after a fixed number of iterations. In what follows we will describe our implementation of two broad types of models: ML regressors and ML classifiers.

We will use a ML regressor whenever we are interested in training a model to predict actual outputs from the calculation of observables. In this case the training requires parameter values and their numerical results from the HEP calculation. When we pass a large number of parameter values we get a set of predictions for the observables, \hat{Y} , that can aid in the selection of the regions of interest. In this case, the K set could be composed of relevant points based on, e.g., χ^2 or likelihood values. However, one could devise any number of selection mechanisms that take advantage of the access to predictions for the observables. The precision of this predictions is expected to be improved with more iterations and this can be easily checked via measures such as the mean absolute error (MAE). After several iterations, using this process should result in a parameter space sampling heavily weighted towards the region of interest used to select the K set and a model specialized in giving accurate and fast predictions for this region.

A different approach would be training a ML classifier to predict if a point in the parameter space would be classified as inside or outside the region of interest according to conditions set by the study being performed. Examples of this conditions would be whether or not the parameter point is theoretically viable and if the point is still inside constraints set by experiments, among several others options. In contrast to the regressor described above, in this case, we expect a binary output from the HEP calculation, say, 1 if the point is inside, 0 if outside. However, after training the ML model, the predictions, \hat{Y} , would be distributed in the range $[0, 1]$. This presents different opportunities for the selection of points, considering that this prediction can be interpreted as how likely a point is to be classified as inside or outside the desired region. A simple choice would be to take K from the points most likely to be inside. Another choice could be taking points around $\hat{Y} = 0.5$, where the model is more uncertain, or even a combination of different ranges. One advantage of already having this classification of points, is that we can try to balance training with sets of equal size for the two classes of points and apply boosting techniques if any class is undersampled. One example of boosting technique is the synthetic minority oversampling technique (SMOTE) [22] that will be explained later in the text. Another advantage of a classification is that it allows the accumulation of a sample of points inside the allowed parameter space in separation from the sample of points outside that needs to be kept to train the model.

In Fig. 1 we show flowcharts of the iterative process followed for both the ML regressor (left) and the ML classifier (right). Both of them start with an initial 0th training step and proceed to the first prediction step inside the iterative steps. The green arrows indicate the places where sets of random parameters have to be inserted and orange arrows indicate the steps where points are accumulated in the sampled parameter space pool.

3 Application to toy models

In this section we apply the iterative process described in the previous section to two simple toy models with 2 and 3 variables. For both models it is possible to choose regions of interest that are completely disconnected and contain a region of low relevance inside. While these two features hardly capture all the complexity that can appear when scanning the parameters of a realistic multidimensional model, in these toy models it is shown how following the processes outlined in the last section easily overcomes these two generic complications.

The simpler model is a 2-dimensional oscillatory surface described by the function

$$O_{2d} = \left[2 + \cos\left(\frac{x_1}{5}\right) \cos\left(\frac{x_2}{7}\right) \right]^5 \quad (1)$$

where our regions of interest will be centered at $c_{2d} = 100$ with an error of $\sigma_{2d} = 100$. The second model depends on three parameters and is given by the function

$$O_{3d} = \left[2 + \cos\left(\frac{x_1}{7}\right) \cos\left(\frac{x_2}{7}\right) \cos\left(\frac{x_3}{7}\right) \right]^5 \quad (2)$$

where we will use a preferred region with center at $c_{3d} = 100$ and a standard deviation of $\sigma_{3d} = 20$. We will take a gaussian likelihood given by $\mathcal{L}_j = \exp[-(O_j - c_j)^2 / 2\sigma_j^2]$ where $j \in \{2d, 3d\}$. These choices of central values and deviations result in ring-shaped and shell-shaped regions of interest for the 2-dimensional and 3-dimensional models, respectively.

For the two toy models we will apply the approaches of regression and classification to illustrate the advantages of each approach and demonstrate the differences in the obtained results. We will

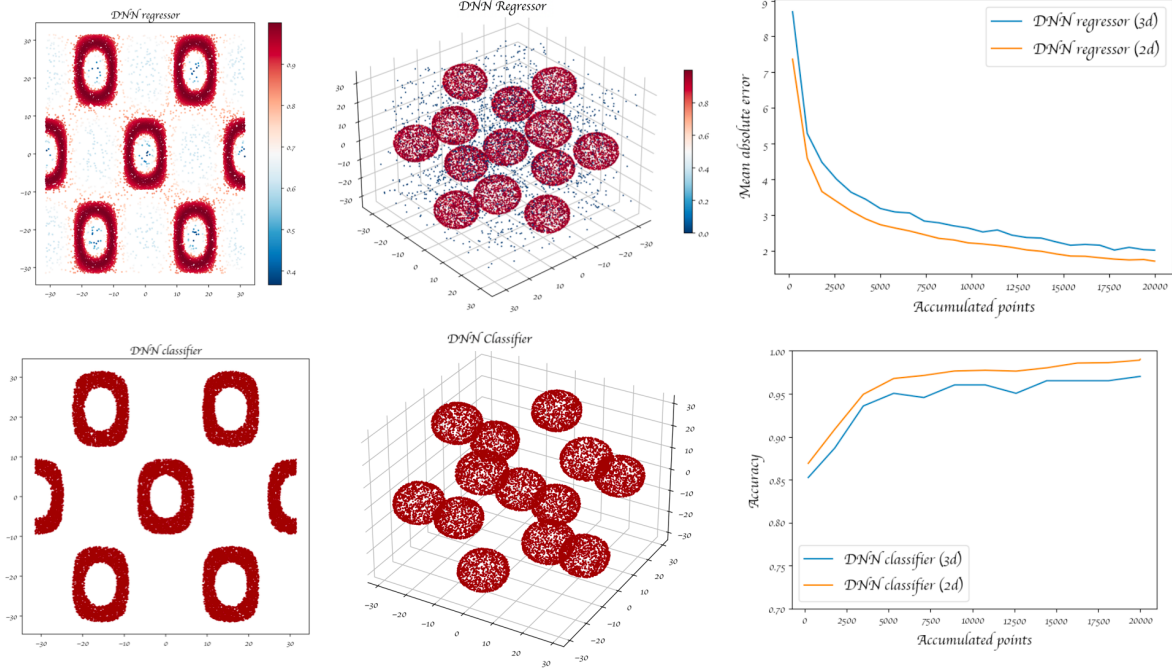


Figure 2: Sampled parameter space using an MLP regressor (upper row) and MLP classifier (lower row) for the toy models in 2 dimensions (left) and 3 dimensions (center). The details of the setup of the MLP are as described in the text. A total of 20 000 accumulated points are shown for all cases. For the upper row, we actively required the MLP to focus on points above a likelihood of 0.9. In the bottom row, a classifier allows for the accumulation of points inside a region of interest ($Y = 1$) without a measure of the quality of the selected points. The MAE of the regressor (the lower the better) as a function of accumulated points is shown in the upper right while we show the accuracy of the classifier (the higher the better) in the lower right.

be using a multi-layer perceptron (MLP) with fully connected layers. The network will have 4 hidden layers, each of them with 100 neurons, and ReLU activation function. The final layer will have one neuron with a linear activation function in the case of the regressor and a sigmoid activation function for the classifier. For the loss function we will use the mean squared error for the regressor and binary cross entropy for the classifier. In both cases we use the Adam optimizer with a learning rate of 0.001, exponential decay rates $\beta_1 = 0.9$ and $\beta_2 = 0.999$, and train during 1000 epochs. For the two toy models and for all the dimensions ($j = 1, 2, 3$) we will scan in the range $x_j \in [-10\pi, 10\pi]$.

To test the ML regressor, we will select the K set using 90% points with a likelihood above 0.9 with the likelihood calculated for the set of predictions \hat{Y} from the ML model. The other 10% will be taken randomly from the parameter space. For training, we will include the accumulated set of points every 2 iterations and in the final iteration to improve the accuracy of the model. When using a regressor, we accumulate all the suggested points which should start to accrue around the region of interest which in our case would be points above the likelihood mentioned before.

For the ML classifier, the selection of the K set will be composed of 90% from points that the model predicts will be inside the region of interest and 10% of points chosen at random. The

condition for a point to be predicted as inside (class $Y = 1$) is that $\hat{Y} > 0.5$. After calculating the actual classification for the suggested points, if the resulting sizes of the groups are imbalanced we apply a boosting method as will be explained in the next part. Every few steps, the training will include points from the pool of accumulated points from both classes, besides the new points found in that step. In this case, the additional points for training will be composed by 50% from the pool of points of each class. Since we have a clear distinction between classes, at the end we report the amount of points accumulated for the class inside the region of interest.

The results from sampling the parameter space for the two toy models using the regressor is shown in the upper row of Fig. 2. In the left pane we show the accumulated points for the toy model defined with Eq. (1) while in the center we show the same for the toy model of Eq. (2). In both figures (upper left and upper center) the color represents the value of the likelihood. For both toy models, it is easy to see that most points accumulate around the regions of interest while a few points are dispersed in the rest of the parameter space. Considering that these points represent the data that was used to train the regressor, we can expect the ML model to be highly specialized in predicting the observables in the region of interest. Note that for the 3-dimensional example, the regions of interest are spherical hollow shells. The upper rightmost panel of Fig. 2 shows the evolution of the MAE (the lower the better), calculated as $\text{MAE} = \sum_{i=1}^n |\hat{Y}_i - Y_i|/n$, for n accumulated points, starting with 100 points. We can see that for the first 2500 points there is a steep reduction in MAE for both toy models. Interestingly, the reduction of the MAE for both models follows a similar trend despite the difference in dimensions, with the MAE for the 3-dimensional model slightly shifted upwards.

For the sampling using the classifier, we show the results of sampling the parameter space in the lower row of Fig. 2. In contrast to the regressor, the sample of parameter values cleanly shows the region of interest, mostly due to the fact that in this case we separately accumulated and displayed the points classified as viable during the calculation. To illustrate the improvement of the ML classifier model after every iteration, in the lower rightmost panel we show the accuracy (the higher the better) as a function of the accumulated points, calculated as the ratio between correct and total number of predictions, starting at 100. Again, this measure follows the same trend for the two toy model examples with the 3-dimensional classifier slightly shifted downwards.

To comment on the most notable difference between the ML regressor and classifier, the fact that the classifier explicitly distinguishes two regions makes possible to operate differently on the points depending on where they have been classified. Above we have decided to display only the accumulated points that were classified inside the region of interest. Additionally, we show that we have control over how we pick up points for the training step from the accumulated pools of the two classes. To expand on the classifier, in the next section we show how we can use a small amount of points to actively balance situations where one of the classes tends to be oversampled.

3.1 Boosting the start up convergence

Unlike the ML regressor, in the case of the ML classifier both classes of points are of equal importance. Accordingly, points outside the region of interest are also accumulated to train the model to find their subspace. Therefore, we train the model using data sets of the same size. When the subspace of points of one class is comparably much smaller than that of the other class, the ML model is inefficient to suggest enough points of the smaller class to pass to the HEP calculation in the initial steps, leading to slow convergence. Moreover, we end up training the model with much more points from one class than the other. There are several ways to rectify this imbalance of the data:

- Undersampling the majority class. In this case we loose much of the information from the undersampled class causing the model to converge very slow.
- Oversampling the minority class by creating random copies from the underrepresented set [16]. This makes the model overestimate the majority class during the test step.
- Oversampling the minority class using SMOTE [22]. The SMOTE transformation is an over-sampling technique in which the minority class is enhanced by creating synthetic samples rather than by oversampling with replacement. This technique involves taking each point from the minority class and introducing synthetic samples along the line segments joining them to their nearest neighbors. Depending on the amount of oversampling required, a number n of nearest neighbors can be randomly chosen. After this, a synthetic sample is generated from the lines between a point and its n nearest neighbors depending on the amount of oversampling required.

The result of oversampling the minority class using SMOTE is shown in Fig. 3 where the minority class (blue points) with 100 points is oversampled to 10 000 points according to the description of the process given above. As mentioned above, we attempt to take a set K made of 90% with predicted $\hat{Y} > 0.5$ expecting that the HEP calculation finds most of them with $Y = 1$, while the other 10% is taken randomly. If the corrected classes, as given by the HEP calculation, have different sizes we use SMOTE to oversample the minority class. The points suggested by SMOTE are then passed to the HEP calculation for proper classification. It is important to mention that the number of the nearest neighbours used by SMOTE is a hyperparameter that has to be adjusted according to the study under consideration. In Fig. 4 we compare the number of accumulated points after 100 iterations when SMOTE is applied (orange) and not applied (blue) to oversample the minority class ($Y = 1$ in this case) and in case of undersampling the majority class. We found that in the case of 2-dimensional toy model, Eq. (1), with initial batch size $K_0 = 3000$, $L = 1000$ and $K = 200$, after 100 iterations the model can accumulate roughly 4 times more points with $Y = 1$ when oversampling using SMOTE compared to not applying any correction method. Similarly, for the 3-dimensional toy model, Eq. (2), with $K_0 = 10\,000$, $L = 3000$ and $K = 200$ the model is able to accumulate 5 times more points when SMOTE is employed.

4 Learning the Higgs signal strength in 2HDM-II potential

In this section we show the performance of ML models scanning over the parameter space of the 2HDM-II scalar potential to match the measured Higgs signal strength.

4.1 The model

In 2HDMs [23,24], the scalar sector contains two $SU(2)_L$ -doublet fields, ϕ_1 and ϕ_2 , with identical quantum numbers under the SM gauge symmetry group:

$$\phi_1 = \begin{pmatrix} \eta_1^+ \\ (v_1 + h_1 + ih_3)/\sqrt{2} \end{pmatrix} \quad \text{and} \quad \phi_2 = \begin{pmatrix} \eta_2^+ \\ (v_2 + h_2 + ih_4)/\sqrt{2} \end{pmatrix}. \quad (3)$$

The components h_i , $i = 1, \dots, 4$, are real neutral fields, η_i^+ , $i = 1, 2$ are complex charged fields, and v_i , $i = 1, 2$ are the vacuum expectation values (vevs). The most general Lagrangian density

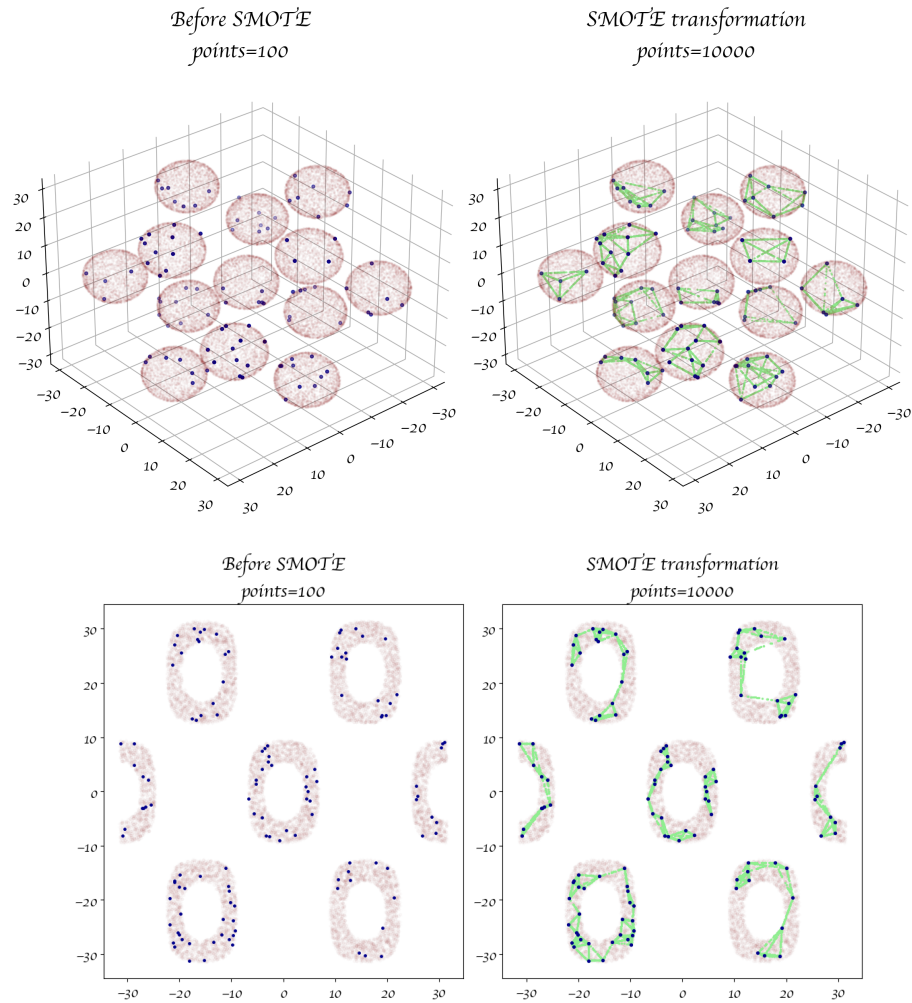


Figure 3: Upper-left and lower-left: The minority class of points inside the region of interest is represented by the blue points while the red points represent the region of interest. Upper-right and lower-right: points from oversampling of the minority class using SMOTE with 3 nearest neighbours are displayed in green.

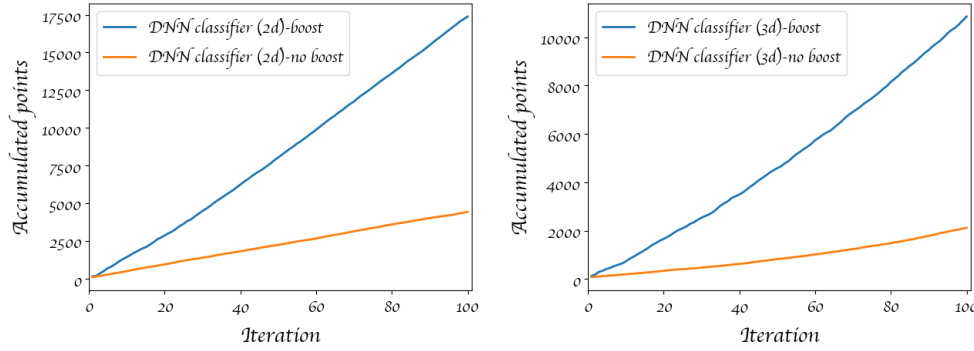


Figure 4: Number of accumulated points in terms of iterations in case of applying (blue) and not applying (orange) the boosting method, for the 2-dimensional (left) and 3-dimensional (right) toy models. The sizes of the sets K_0 , L and K as well as details for the selection of points are described in the text.

for the model can be decomposed as

$$\mathcal{L}_{\text{2HDM}} = \mathcal{L}_{\text{SM,kin}} + \mathcal{L}_{\phi,\text{kin}} + V_\phi + Y_\phi, \quad (4)$$

where $\mathcal{L}_{\text{SM,kin}}$ denotes the kinetic terms for SM gauge fields and fermions, $\mathcal{L}_{\phi,\text{kin}}$ denotes the kinetic terms for the two scalar fields ϕ_i , $i = 1, 2$, V_ϕ denotes the scalar potential, and Y_ϕ contains the Yukawa terms that give rise to the couplings between the SM fermions and the scalar fields. The scalar potential with a softly broken Z_2 symmetry is given by

$$\begin{aligned} V_\phi = & m_{11}^2(\phi_1^\dagger\phi_1) + m_{22}^2(\phi_2^\dagger\phi_2) - [m_{12}^2(\phi_1^\dagger\phi_2) + h.c.] + \lambda_1(\phi_1^\dagger\phi_1)^2 + \lambda_2(\phi_2^\dagger\phi_2)^2 \\ & + \lambda_3(\phi_1^\dagger\phi_1)(\phi_2^\dagger\phi_2) + \lambda_4(\phi_1^\dagger\phi_2)(\phi_2^\dagger\phi_1) + \frac{1}{2}[\lambda_5(\phi_1^\dagger\phi_2)^2 + H.c.]. \end{aligned} \quad (5)$$

The parameters m_{ii}^2 , $\lambda_{i \neq 5}$ are real. The possible complex phases that allow for CP violation belong to the two parameters $m_{12}^2 = |m_{12}^2|e^{i\eta(m_{12}^2)}$ and $\lambda_5 = |\lambda_5|e^{i\eta(\lambda_5)}$ [30, 31]. The tadpole equations impose a relation between the two complex phases, such that the CP violation can be parametrised ultimately via the parameter $\eta(\lambda_5)$, the complex phase of λ_5 . In the following we consider real potential with $\eta(\lambda_5) = 0$. Moreover, The vacuum expectation values for the two doublet fields satisfy $v = \sqrt{v_1^2 + v_2^2}$, with v denoting the SM vev $v \sim 246$ GeV, and we define $\tan\beta \equiv v_2/v_1$.

The Z_2 -symmetric Yukawa terms of type-II 2HDM are given by

$$-\mathcal{L}_Y = Y_u \overline{Q_L} \tilde{\phi}_2 u_R + Y_d \overline{Q_L} \phi_2 d_R + Y_l \overline{L_L} \phi_2 l_R + H.c., \quad (6)$$

where $\tilde{\phi}_2 = i\tau_2\phi_2^*$ and Y_u, Y_d, Y_l are the 3×3 Yukawa matrices.

We perform a scan over six free parameters of the potential, λ_j ($j \in \{1, 2, 3, 4, 5\}$) and $\tan\beta$, to adjust the SM-like Higgs properties to match current measurements. Note that one has the freedom to scan over physical parameters instead. Each parameter base has their own advantages, for example, using parameters of the potential allows to choose ranges where stability and perturbativity test are automatically passed. We use SPHeno-4.0.5 [25] to calculate the particles spectrum of the physical eigenstates while HiggsBounds-5.3.2 [26, 27] and HiggsSignals-2.2.3 [28, 29] are used to constraint the parameter space using recent Higgs boson measurements. HiggsBounds

first identifies the most sensitive signal channel for each scalar, H_i , separately and then computes the ratio of this theoretical prediction to the observed signal strength for heavy/light scalars as

$$\mathcal{O}_i = \frac{\sigma \times \text{BR}(H_i)_{\text{models}}}{\sigma \times \text{BR}(H_i)_{\text{obs}}} \quad (7)$$

which we use to obtain an exclusion limit at 95% C.L. if $\mathcal{O}_i > 1$. Additionally, HiggsSignals evaluates the statistical compatibility of the lightest SM-like Higgs boson in the model with the observed scalar resonance, as it was observed by LHC run-I and run-II experiments. A χ^2 test for the model hypothesis is performed as a combination from the χ_μ^2 from the signal strength modifiers and the corresponding predicted Higgs masses as

$$\chi_{\text{tot}}^2 = \chi_\mu^2 + \sum_{i=1}^{N_H} \chi_{m_{H_i}}^2. \quad (8)$$

The best fit value is calculated according to

$$\chi_{\text{best}}^2 = \chi_{\text{min}}^2 / n_{\text{D.O.F.}} \quad (9)$$

with χ_{min}^2 the minimum χ^2 . We adjust our selection to accept all points with $\chi_{\text{tot}}^2 \leq 95$. It is worth mentioning that all selected points are required to pass the HiggsBounds selection.

During testing, we observed that the ML regressor model requires less initial points in cases where the likelihood is less peaked or less fast changing. Therefore, we consider the following narrow ranges:

$$\begin{aligned} 0.1 \leq \lambda_1 \leq 0.5, & \quad 0.1 \leq \lambda_2 \leq 0.2, & \quad -0.1 \leq \lambda_3 \leq -0.5, \\ 5 \leq \lambda_4 \leq 6.5, & \quad -6.5 \leq \lambda_5 \leq -6, & \quad 30 \leq \tan \beta \leq 35, \end{aligned} \quad (10)$$

with $m_{12}^2 = -2500 \text{ GeV}^2$. We use a sequential MLP with four hidden layers each with 100 neurons and ReLU activation function. The final output layer contains only one neuron with linear activation function. The loss function in this case is the mean squared error which is minimized by Adam optimizer with learning rate of 0.001 and exponential decay rates $\beta_1 = 0.9$ and $\beta_2 = 0.999$. We train during 1000 epochs in every step. The collected samples are fully utilized to train the ML model after every two iterations, without validation and test samples, since calculating observables precisely using HEP packages is time consuming. We accumulate 20 000 points after 345 iteration with initial batch size $K_0 = 50\,000$, $L = 10\,000$ and $K = 200$ with 10% random points. We sampled the batch K from the ML predictions as 90% of the points with $\chi^2 \leq 95$ and 10% random points. These points are then passed to the HEP packages to be corrected to their true values. In Fig. 5 we show the pattern of 20 000 accumulated points during the sampling process for the scanned parameters of the potential. It is pretty clear that most of the points are concentrated in the region that satisfy the $\chi^2 \leq 95$. Additionally, there is a number of randomly distributed points that perfectly span the full parameter space to ensure that we do not miss any subspace that may satisfy the χ^2 condition. It is important to mention that, after the sampling process, one can use the trained model to predict the output of new points in the region of interest without calling the HEP package while retaining a very good accuracy.

Since the ML classifier is less affected by fast changing or peaked likelihoods than the regressor we can consider wider ranges without a dramatic increase in the number of points. Therefore, in this case we scan over the following ranges

$$\begin{aligned} 0 \leq \lambda_1 \leq 1, & \quad 0 \leq \lambda_2 \leq 1, & \quad -0.5 \leq \lambda_3 \leq 0, \\ 0 \leq \lambda_4 \leq 7, & \quad 8 \leq \lambda_5 \leq -2, & \quad 20 \leq \tan \beta \leq 40, \end{aligned} \quad (11)$$

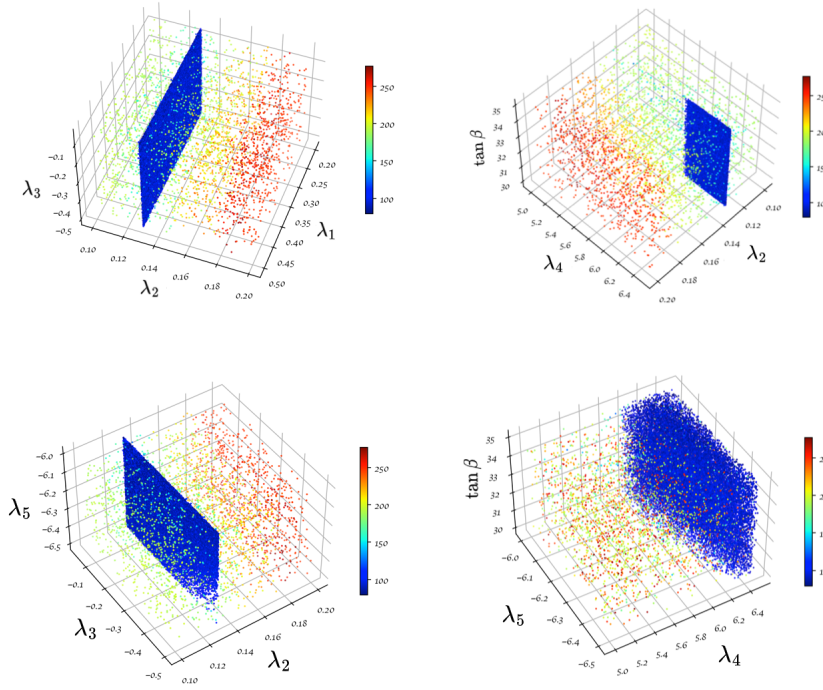


Figure 5: Accumulated points from MLP regressor model. The color bar represents the χ^2 reported by the HiggsSignals package.

with $m_{12}^2 = -2500 \text{ GeV}^2$. We use a sequential MLP with four hidden layers with 100 neurons in each layer and ReLU activation function. The output layer has one neuron with Sigmoid activation which maps the output to probability ranges between 0 and 1. We train during 1000 epochs. In each iteration we select the K points from the ML predictions similar to the ML regressor method. The sampled K points are then passed to the HEP packages to classify them. In the steps where the data sets are imbalanced, SMOTE is automatically called to oversample the minority class. Also, the training data are normalized according to the standard normal distribution. Indeed normalizing the inputs before fitting the MLP model is important to ensure the convergence of the model to a global minimum of the loss function.² Figure 6 shows the pattern of accumulated 20 000 good points from 170 iteration and initial batch size $K_0 = 50\,000$, $L = 10\,000$ and $K = 200$ points with 10% random points.

5 Conclusion

In this paper we have discussed the implementation of two broad types of ML based approaches for the efficient sampling of multidimensional parameter spaces: regression and classification. The ML model is employed as part of an iterative process where it is used to suggest new points and trained according to the results of this suggestion. In the case of the regression we train a ML model to precisely predict observables in regions favoured by observations. For the classification

²MLP model is very sensitive to the ranges of the input features and we have to normalize the input before we use it to fit the model. On the other hand other models, like random forest, are robust against the outliers and can be used without normalization of the input features.

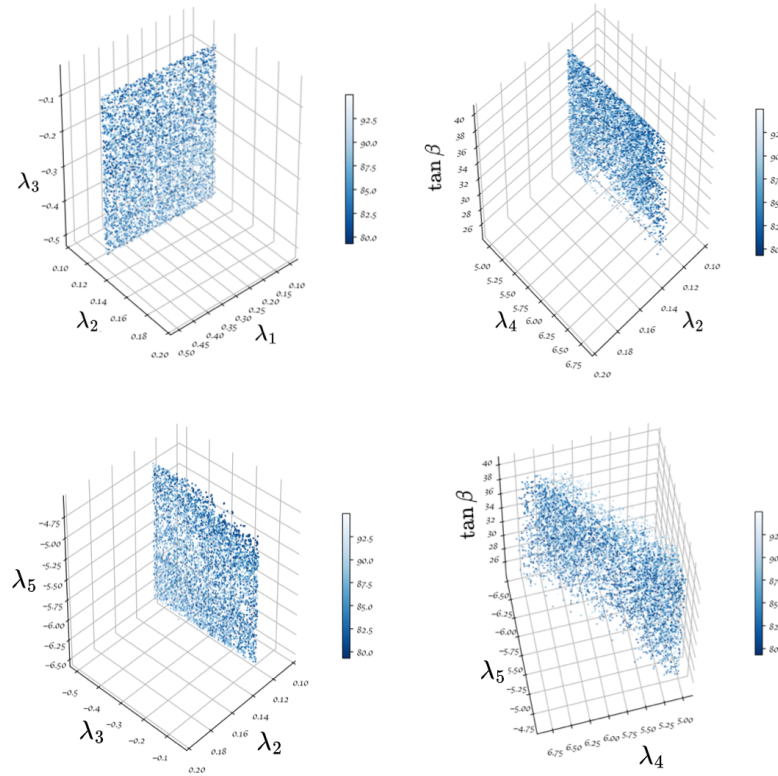


Figure 6: MLP classifier model with 20 000 points. The color bar represents the χ^2 reported by the HiggsSignals package.

we train the model to be able to separate the points that belong to the region of interest from those outside of it. In the case of the classification we devise a process to alleviate undersampling of small regions employing SMOTE. We find that both approaches can efficiently sample regions of interest with features like several disconnected regions or regions of low interest inside regions of high interest. In particular, we applied the two types of model to toy models in 2 and 3 dimensions and found that in both cases the accuracy of the trained model follows the same trend. For the classification model we found that using SMOTE to balance the sampling of the two classes can considerably improve the accumulation of points inside regions of interest when compared to not applying any balancing method. To finalize, we sampled the parameter space of the 2HDM by integrating our iterative implementation with popular HEP packages that take care of calculating the theoretical and experimental results. We found that we can accumulate points on regions of interest, defined by χ^2 ranges, even when some parameters are narrowly distributed inside the scanned region. With the two types of model, in a few hundred iterations we are able to collect 20 000 points densely distributed in the regions with the lowest χ^2 . However, this implementation may still face difficulties when the number of dimensions is too large and/or when the regions of interest are very narrowly distributed so that in the first steps the random samples hardly contain any usable points. The code employed to calculate the examples presented here is freely available on the web³.

Acknowledgements

This work is supported by NRF-2021R1A2C4002551. PS is also supported by the Seoul National University of Science and Technology.

References

- [1] R. L. Workman [Particle Data Group], “Review of Particle Physics,” PTEP **2022**, 083C01 (2022) doi:[10.1093/ptep/ptaa104](https://doi.org/10.1093/ptep/ptaa104).
- [2] D.J.C. MacKay, “Information Theory, Inference and Learning Algorithms,” Cambridge University Press, 2003.
- [3] F. Feroz and M. P. Hobson, “Multimodal nested sampling: an efficient and robust alternative to MCMC methods for astronomical data analysis,” Mon. Not. Roy. Astron. Soc. **384**, 449 (2008) doi:[10.1111/j.1365-2966.2007.12353.x](https://doi.org/10.1111/j.1365-2966.2007.12353.x) [arXiv:0704.3704 [astro-ph]].
- [4] F. Feroz, M. P. Hobson and M. Bridges, “MultiNest: an efficient and robust Bayesian inference tool for cosmology and particle physics,” Mon. Not. Roy. Astron. Soc. **398**, 1601-1614 (2009) doi:[10.1111/j.1365-2966.2009.14548.x](https://doi.org/10.1111/j.1365-2966.2009.14548.x) [arXiv:0809.3437 [astro-ph]].
- [5] A. Lewis and S. Bridle, “Cosmological parameters from CMB and other data: A Monte Carlo approach,” Phys. Rev. D **66**, 103511 (2002) doi:[10.1103/PhysRevD.66.103511](https://doi.org/10.1103/PhysRevD.66.103511) [arXiv:astro-ph/0205436 [astro-ph]].

³<https://github.com/AHamamd150/MLscanner>

- [6] R. Lafaye, T. Plehn and D. Zerwas, “SFITTER: SUSY parameter analysis at LHC and LC,” [arXiv:hep-ph/0404282 [hep-ph]].
- [7] P. Bechtle, K. Desch and P. Wienemann, “Fittino, a program for determining MSSM parameters from collider observables using an iterative method,” *Comput. Phys. Commun.* **174**, 47-70 (2006) doi:[10.1016/j.cpc.2005.09.002](https://doi.org/10.1016/j.cpc.2005.09.002) [arXiv:hep-ph/0412012 [hep-ph]].
- [8] R. Ruiz de Austri, R. Trotta and L. Roszkowski, “A Markov chain Monte Carlo analysis of the CMSSM,” *JHEP* **05**, 002 (2006) doi:[10.1088/1126-6708/2006/05/002](https://doi.org/10.1088/1126-6708/2006/05/002) [arXiv:hep-ph/0602028 [hep-ph]].
- [9] B. C. Allanach and C. G. Lester, “Sampling using a ‘bank’ of clues,” *Comput. Phys. Commun.* **179**, 256-266 (2008) doi:[10.1016/j.cpc.2008.02.020](https://doi.org/10.1016/j.cpc.2008.02.020) [arXiv:0705.0486 [hep-ph]].
- [10] C. Strege, G. Bertone, G. J. Besjes, S. Caron, R. Ruiz de Austri, A. Strubig and R. Trotta, “Profile likelihood maps of a 15-dimensional MSSM,” *JHEP* **09**, 081 (2014) doi:[10.1007/JHEP09\(2014\)081](https://doi.org/10.1007/JHEP09(2014)081) [arXiv:1405.0622 [hep-ph]].
- [11] C. Han, K. i. Hikasa, L. Wu, J. M. Yang and Y. Zhang, “Status of CMSSM in light of current LHC Run-2 and LUX data,” *Phys. Lett. B* **769**, 470-476 (2017) doi:[10.1016/j.physletb.2017.04.026](https://doi.org/10.1016/j.physletb.2017.04.026) [arXiv:1612.02296 [hep-ph]].
- [12] P. Athron *et al.* [GAMBIT], “GAMBIT: The Global and Modular Beyond-the-Standard-Model Inference Tool,” *Eur. Phys. J. C* **77**, no.11, 784 (2017) doi:[10.1140/epjc/s10052-017-5321-8](https://doi.org/10.1140/epjc/s10052-017-5321-8) [arXiv:1705.07908 [hep-ph]].
- [13] E. Bagnaschi, K. Sakurai, M. Borsato, O. Buchmueller, M. Citron, J. C. Costa, A. De Roeck, M. J. Dolan, J. R. Ellis and H. Flücher, *et al.* “Likelihood Analysis of the pMSSM11 in Light of LHC 13-TeV Data,” *Eur. Phys. J. C* **78**, no.3, 256 (2018) doi:[10.1140/epjc/s10052-018-5697-0](https://doi.org/10.1140/epjc/s10052-018-5697-0) [arXiv:1710.11091 [hep-ph]].
- [14] T. Brinckmann and J. Lesgourgues, “MontePython 3: boosted MCMC sampler and other features,” *Phys. Dark Univ.* **24**, 100260 (2019) doi:[10.1016/j.dark.2018.100260](https://doi.org/10.1016/j.dark.2018.100260) [arXiv:1804.07261 [astro-ph.CO]].
- [15] J. Ren, L. Wu, J. M. Yang and J. Zhao, “Exploring supersymmetry with machine learning,” *Nucl. Phys. B* **943**, 114613 (2019) doi:[10.1016/j.nuclphysb.2019.114613](https://doi.org/10.1016/j.nuclphysb.2019.114613) [arXiv:1708.06615 [hep-ph]].
- [16] M. D. Goodsell and A. Joury, “Active learning BSM parameter spaces,” [arXiv:2204.13950 [hep-ph]].
- [17] M. Feickert and B. Nachman, “A Living Review of Machine Learning for Particle Physics,” [arXiv:2102.02770 [hep-ph]].
- [18] F. Staub, “xBIT: an easy to use scanning tool with machine learning abilities,” [arXiv:1906.03277 [hep-ph]].
- [19] S. Caron, T. Heskes, S. Otten and B. Stienen, “Constraining the Parameters of High-Dimensional Models with Active Learning,” *Eur. Phys. J. C* **79**, no.11, 944 (2019) doi:[10.1140/epjc/s10052-019-7437-5](https://doi.org/10.1140/epjc/s10052-019-7437-5) [arXiv:1905.08628 [cs.LG]].

- [20] J. Rocamonde, L. Corpe, G. Zilgalvis, M. Avramidou and J. Butterworth, “Picking the low-hanging fruit: testing new physics at scale with active learning,” *SciPost Phys.* **13**, 002 (2022) doi:[10.21468/SciPostPhys.13.1.002](https://doi.org/10.21468/SciPostPhys.13.1.002) [arXiv:2202.05882 [hep-ph]].
- [21] F. A. de Souza, M. Crispim Romão, N. F. Castro, M. Nikjoo and W. Porod, “Exploring Parameter Spaces with Artificial Intelligence and Machine Learning Black-Box Optimisation Algorithms,” [arXiv:2206.09223 [hep-ph]].
- [22] N. V. Chawla, K. W. Bowyer, L. O. Hall and W. P. Kegelmeyer, “SMOTE: Synthetic Minority Over-sampling Technique,” *Journal of Artificial Intelligence Research* **16** (2002) 321–357 doi:[10.1613/jair.953](https://doi.org/10.1613/jair.953) [arXiv:1106.1813 [hep-ph]].
- [23] T. D. Lee, “A Theory of Spontaneous T Violation,” *Phys. Rev. D* **8**, 1226-1239 (1973) doi:[10.1103/PhysRevD.8.1226](https://doi.org/10.1103/PhysRevD.8.1226)
- [24] G. C. Branco, P. M. Ferreira, L. Lavoura, M. N. Rebelo, M. Sher and J. P. Silva, “Theory and phenomenology of two-Higgs-doublet models,” *Phys. Rept.* **516**, 1-102 (2012) doi:[10.1016/j.physrep.2012.02.002](https://doi.org/10.1016/j.physrep.2012.02.002) [arXiv:1106.0034 [hep-ph]].
- [25] W. Porod and F. Staub, “SPHeno 3.1: Extensions including flavour, CP-phases and models beyond the MSSM,” *Comput. Phys. Commun.* **183** (2012), 2458-2469 doi:[10.1016/j.cpc.2012.05.021](https://doi.org/10.1016/j.cpc.2012.05.021) [arXiv:1104.1573 [hep-ph]].
- [26] P. Bechtle, O. Brein, S. Heinemeyer, G. Weiglein and K. E. Williams, “HiggsBounds: Confronting Arbitrary Higgs Sectors with Exclusion Bounds from LEP and the Tevatron,” *Comput. Phys. Commun.* **181** (2010), 138-167 doi:[10.1016/j.cpc.2009.09.003](https://doi.org/10.1016/j.cpc.2009.09.003) [arXiv:0811.4169 [hep-ph]].
- [27] P. Bechtle, O. Brein, S. Heinemeyer, G. Weiglein and K. E. Williams, “HiggsBounds 2.0.0: Confronting Neutral and Charged Higgs Sector Predictions with Exclusion Bounds from LEP and the Tevatron,” *Comput. Phys. Commun.* **182** (2011), 2605-2631 doi:[10.1016/j.cpc.2011.07.015](https://doi.org/10.1016/j.cpc.2011.07.015) [arXiv:1102.1898 [hep-ph]].
- [28] P. Bechtle, S. Heinemeyer, O. Stål, T. Stefaniak and G. Weiglein, “*HiggsSignals*: Confronting arbitrary Higgs sectors with measurements at the Tevatron and the LHC,” *Eur. Phys. J. C* **74** (2014) no.2, 2711 doi:[10.1140/epjc/s10052-013-2711-4](https://doi.org/10.1140/epjc/s10052-013-2711-4) [arXiv:1305.1933 [hep-ph]].
- [29] O. Stål and T. Stefaniak, “Constraining extended Higgs sectors with HiggsSignals,” *PoS EPS-HEP2013* (2013), 314 doi:[10.22323/1.180.0314](https://doi.org/10.22323/1.180.0314) [arXiv:1310.4039 [hep-ph]].
- [30] S. Antusch, O. Fischer, A. Hammad and C. Scherb, “Testing CP Properties of Extra Higgs States at the HL-LHC,” *JHEP* **03** (2021), 200 doi:[10.1007/JHEP03\(2021\)200](https://doi.org/10.1007/JHEP03(2021)200) [arXiv:2011.10388 [hep-ph]].
- [31] S. Antusch, O. Fischer, A. Hammad and C. Scherb, “Explaining excesses in four-leptons at the LHC with a double peak from a CP violating Two Higgs Doublet Model,” [arXiv:2112.00921 [hep-ph]].